THE JOURNAL OF BIOLOGICAL CHEMISTRY VOL. 286, NO. 6, pp. 4912–4921, February 11, 2011

Preconditioning with Endoplasmic Reticulum Stress Mitigates Retinal Endothelial Inflammation via Activation of X-box Binding Protein 1*

Received for publication, November 1, 2010 Published, JBC Papers in Press, December 7, 2010, DOI 10.1074/jbc.M110.199729

Jingming Li[‡§], Joshua J. Wang[‡§], and Sarah X. Zhang[‡§¶1]

From the [‡]Department of Medicine, Endocrinology and Diabetes, the [§]Harold Hamm Oklahoma Diabetes Center, [¶]Oklahoma Center for Neuroscience, University of Oklahoma Health Sciences Center, Oklahoma City, Oklahoma 73104

Endoplasmic reticulum (ER) stress is widely implicated in various pathological conditions such as diabetes. Previously, we reported that enhanced ER stress contributes to inflammation and vascular damage in diabetic and ischemia-induced retinopathy. However, the exact role of the signaling pathways activated by ER stress in vascular inflammation remains poorly understood. In the present study, we investigated the role of X-box binding protein 1 (XBP1) in retinal adhesion molecule expression, leukostasis, and vascular leakage. Exposure of human retinal endothelial cells to low dose ER stress inducers resulted in a robust activation of XBP1 but did not affect inflammatory gene expression. However, ER stress preconditioning almost completely abolished TNF-α-elicited NF-κB activation and adhesion molecule ICAM-1 and VCAM-1 expression. Pharmaceutical inhibition of XBP1 activation or knockdown of XBP1 by siRNA markedly attenuated the effects of preconditioning on inflammation. Moreover, loss of XBP1 led to an increase in ICAM-1 and VCAM-1 expression. Conversely, overexpression of spliced XBP1 attenuated TNF-α-induced phosphorylation of IKK, IκBα, and NF-κB p65, accompanied by decreased NF-κB activity and reduced adhesion molecule expression. Finally, *in vivo* studies show that activation of XBP1 by ER stress preconditioning prevents TNF-α-induced ICAM-1 and VCAM-1 expression, leukostasis, and vascular leakage in mouse retinas. These results collectively indicate a protective effect of ER stress preconditioning against retinal endothelial inflammation, which is likely through activation of XBP1-mediated unfolded protein response (UPR) and inhibition of NF-κB activation.

Diabetic retinopathy is a major complication of diabetes characterized by progressive damage of retinal microvasculature, disturbed blood supply, and retinal neuronal degeneration (1–4). One important function of retinal vascular system is to form the inner blood-retinal barrier (BRB).[2] The inner BRB, composed of tight junctions between endothelial cells, selectively transport blood content into the retina and thus play an important role in maintaining retinal homeostasis and normal visual activity (5). Breakdown of the BRB due to endothelial cell injury is an early pathological event in diabetic retinopathy (6–9). Impaired endothelial barrier allows macromolecules (proteins and lipids) and fluid leaking from blood vessels into retinal tissues, resulting in diabetic macular edema, the most frequent cause of vision impairment in patients with diabetes.

A growing body of evidence suggests that leukocyte adhesion to endothelial cells and stasis in retinal vasculature (leukostasis) plays a causal role in BRB breakdown (10, 11). Binding of leukocytes to adhesion molecules on the surface of endothelial cells is required for leukostasis (12). During diabetes, endothelial cells are activated and express high levels of adhesion molecules (12, 13). In patients with diabetic retinopathy, levels of soluble intercellular adhesion molecule-1 (ICAM-1) and vascular adhesion molecule-1 (VCAM-1) in the vitreous are drastically enhanced(14), accompanied by increased inflammatory cells, including neutrophils, macrophages, and $CD4^+$ and $CD8^+$ T lymphocytes, in retinal blood vessels (15). Genetic depletion of ICAM-1 or its ligand abolishes retinal leukostasis and protects vascular cells from diabetes-induced apoptosis and vascular leakage (12). Similarly, inhibition of VCAM-1 reduces leukocyte adhesion and rolling in micro- and macrocirculations (16, 17), suggesting that increased expression of adhesion molecules in endothelial cells is critical for leukostasis-mediated vascular injury. Among many potent stimulators of adhesion molecules, TNF-α is a major proinflammatory cytokine induced by diabetes in the retinal vascular system (18). Exposure of retinal endothelial cells to TNF-α induces rapid activation of NF-κB and increased expression of ICAM-1 in parallel with tight junction damage (7). Inhibition of TNF-α function reduces leukostasis-associated retinal vascular leakage (11) and ameliorates capillary nonperfusion in diabetic retinas (19), suggesting an im-

* This work was supported, in whole or in part, by National Institutes of Health Grants EY019949 and P20RR024215. This work was also supported by Research Award 5-2009-475 from the Juvenile Diabetes Research Foundation, Research Grants HR07-167 and HR10-060 from the Oklahoma Center for the Advancement of Science and Technology, Research Grant M2010088 from the American Health Assistance Foundation, and the Dr. William Talley Research Award from the Harold Hamm Oklahoma Diabetes Center.

[1] To whom correspondence should be addressed: 941 Stanton L. Young Blvd., BSEB331A, Oklahoma City, OK 73104. Fax: 405-271-3973; E-mail: xin-zhang@ouhsc.edu.

[2] The abbreviations used are: BRB, blood-retinal barrier; ER, endoplasmic reticulum; IKK, IκB kinase; ICAM-1, intercellular adhesion molecule-1; VCAM-1, vascular adhesion molecule-1; HREC, human retinal microvascular endothelial cell(s); Ad, adenovirus; XBP1, X-box binding protein 1; UPR, unfolded protein response; DME, diabetic macular edema; IRE1, inositol-requiring transmembrane kinase 1; MCP-1, monocyte chemoattractant protein-1; GRP78, 78-kDa glucose-regulated protein.

portant role of TNF-α in retinal inflammation and endothelial cell injury in diabetic retinopathy.

The endoplasmic reticulum (ER) is the principle cellular organelle responsible for proper folding and processing of transmembrane, secretory, or cell-surface proteins. Perturbed ER function results in accumulation of unfolded or misfolded proteins in the ER, a state known as ER stress. Recently, we reported that ER stress plays a pathogenic role in retinal inflammation and vascular leakage in diabetic retinopathy (8). Prolonged ER stress also triggers the apoptotic cascade resulting in cell death (20). Intriguingly, in contrast to the evidence showing the detrimental effects of ER stress, a series of recent studies show that preconditioning with ER stress protects cells against damage induced by oxidative stress and hypoxia (21–24). In a renal disease model, pretreatment of rats with a subnephritogenic dose of ER stress inducers, tunicamycin or thapsigargin, for 4 days ameliorated glomerular histologic damage and proteinuria (21). Moreover, priming of renal mesangial cells with ER stress inducers resulted in blunted induction of monocyte chemoattractant protein-1 (MCP-1) in response to inflammatory stimuli (24). These studies strongly suggest a cytoprotective role of signal pathways activated by ER stress; however, the mechanisms are yet to be investigated.

In the present study, we examined the effect and mechanism of ER stress preconditioning on cytokine-induced inflammation in retinal endothelial cells. We demonstrated that ER stress preconditioning alleviates TNF-α-induced endothelial adhesion molecule expression, retinal leukostasis, and vascular leakage. This process requires activation of X-box binding protein 1 (XBP1), a master coordinator of the adaptive unfolded protein response (UPR). XBP1 negatively regulates inositol-requiring transmembrane kinase 1 IRE1α phosphorylation and suppresses TNF-α-induced activation of the IRE1α/IKK/NF-κB pathway. These findings suggest that improving the function of the ER protective system could be a potential therapeutic strategy to prevent vascular inflammation and retinal damage in diabetes.

EXPERIMENTAL PROCEDURES

Animals—C57BL/6J mice were purchased from the The Jackson Laboratory (Bar Harbor, MI). Care, use, and treatment of all animals in this study were in strict agreement with the Statement for the Use of Animals in Ophthalmic and Vision Research from the Association for Research in Vision and Ophthalmology and with the guidelines set forth by the University of Oklahoma.

Cell Culture—Primary human retinal microvascular endothelial cells (HREC) were obtained from Cell Systems, Inc. (Kirkland, WA) and cultured in EGM-2 supplemented with EGM-2 SingleQuots (Lonza, Walersville, MD). THP-1 cells were obtained from ATCC (Manassas, VA) and maintained in RPMI 1640 medium with 10% fetal bovine serum and 0.05 mM 2-mercaptoethanol. Confluent monolayer HREC were quiescent in medium with 2% FBS for 16 h followed by treatment with the desired conditions. All experiments were conducted with cells at passage 3 to 8. Quinotrierixin was kindly provided by Dr. Tashiro (Keio University). Tunicamycin and thapsigargin were obtained from Sigma-Aldrich. Human TNF-α protein was purchased from PeproTech, Inc. (Rocky Hill, NJ).

Ocular Treatment and Retinal Preparation in Mice—Adult C57BL/6J mice were anesthetized and received pretreatment of tunicamycin (10 ng/eye) in one eye by periocular injection. Same volume of vehicle was injected into the contralateral eye as control. Periocular injection was performed as described previously (25). Twelve hours after pretreatment, mice were randomly assigned to receive an intravitreal injection of TNF-α (1 pmol/eye) or vehicle in both eyes using an UltraMicroPump (World Precision Instruments, Sarasota, FL) (26). Twenty-four hours after injection, mice were subjected to retinal vascular permeability or leukostasis assays or humanly sacrificed, and eyes were enucleated. Retinas were carefully dissected under an operating microscope, flash frozen with liquid nitrogen, and stored at -80 °C for analysis.

Measurement of Retinal Vascular Permeability—Retinal vascular permeability was quantified by measurement albumin leakage from blood vessels into the retina using the Evans blue-albumin method, as described previously (6). Protein concentration was quantified by BCA protein assay (Pierce). Results were expressed as micrograms of Evans blue per milligram of total protein.

Retinal Leukostasis Assay—Retinal leukostasis was determined by labeling retinal vasculature and adherent leukocytes with Alexa Fluor 594-conjugated concanavalin A lectin as described previously (12). Briefly, animals were deeply anesthetized, the chest cavity was opened, and the descending aorta was clamped. A 23-gauge cannula was inserted into the left ventricle. The animals were perfused with PBS to remove erythrocytes and nonadherent leukocytes, followed by concanavalin A (20 μg/ml in PBS (pH 7.4), 5 mg/kg body weight) to label adherent leukocytes and vascular endothelial cells. The retinas were carefully removed, fixed with 4% paraformaldehyde, and flat mounted. Retinal vasculature and adherent leukocytes were imaged with an Olympus Provis AX-70 fluorescent microscope (Olympus, Germany), and the number of adherent leukocytes per retina was determined.

Adenovirus Infection of HREC—Recombinant adenovirus expressing spliced XBP1 (Ad-XBP1S) was generated as described elsewhere (27). Adenovirus expressing GFP (Ad-GFP) was used as control (28). Subconfluent HREC were grown in EGM-2 with SingleQuots and infected by adenovirus at a multiplicity of infection of 20. Forty-eight hours after infection, cells were quiescent with EBM-2 containing 2% FBS for 16 h before experiments.

RNA Interference and Cell Transfection—High performance purity grade (>90% pure) siRNAs were generated against human XBP1 (Qiagen, Valencia, CA). A nonsilencing siRNA oligonucleotide sequence that does not recognize any known homology to mammalian genes was also generated as a negative control. Cells were transfected with siRNA using Lipofectamine 2000 (Invitrogen) as described previously (28). The knockdown efficiency was monitored by determining the protein level of XBP1 using Western blot analysis.

In Vitro Leukocyte Adhesion Assay—HREC were grown to confluence in six-well plates. After preconditioning with tunicamycin or adenoviral infection, HREC were exposed to

TNF-α for 4 h. THP-1 monocytes were directly added to HREC and co-cultured for 3 h. Unbound THP-1 monocytes were removed by washing with PBS for three times, and bound THP-1 monocytes were counted from three different visual fields under a light microscope (Olympus, Germany).

Real-time RT-PCR—Total RNA was extracted using the RNeasy Mini Kit (Qiagen) according to the manufacturer's protocol. Real-time RT-PCR was performed using the iScript cDNA Synthesis kit and SYBR® Green PCR Master Mix (Bio-Rad) as described (28). Specific primers used for real-time PCR are as follows: human ICAM-1 (forward) 5′-TAAGCCAAGAGGAAGGAGCA-3′ and (reverse) 5′-CATATCATCAAGGGTTGGGG-3′; VCAM-1 (forward) 5′-GCTGCTCAGATTGGAGACTCA-3′ and (reverse) 5′-CGCTCAGAGGGCTGTCTATC-3′. The levels of target genes were normalized by 18 S ribosomal RNA. RT-PCR primers used for XBP1 splicing are 5′-TTACGAGAGAAAACTCATGGC-3′ and 5′-GGGTCCAAGTTGTCCAGAATGC-3′. RT-PCR was performed as described previously (29).

Western Blot Analysis—Retinas and cells were lysed in radioimmune precipitation assay buffer with protease inhibitor mixture, PMSF, and sodium orthovanadate (Santa Cruz Biotechnology, Santa Cruz, CA). Twenty-five μg of protein were resolved by SDS-PAGE and then blotted with specific antibodies: anti-ICAM-1, anti-VCAM-1, anti-IκB-β, anti-XBP1 (Santa Cruz Biotechnology), anti-spliced XBP1 (Biolegend, San Diego, CA), anti-inducible nitric oxide synthase, anti-nucleoporin P62 (BD Biosciences), antiphospho-NF-κB p65 (Ser^{536}), anti-NF-κB, phospho-IκB-α (Ser^{32}), anti-IκB-α, antiphospho-IKKα/β ($Ser^{176/180}$) (Cell Signaling Technology, Boston, MA), antiphospho-IRE1α, anti-GRP78 (Abcam, Cambridge, MA), and anti-IRE1α (Novus Biological, Littleton, CO) antibodies. The same membrane was stripped and reblotted with an anti-β-actin antibody (Abcam) as loading control.

NF-κB p65 Transcription Factor Activity Assay—To quantify NF-κB activation, the activity of p65, a subunit of NF-κB, was assayed by the DNA binding capacity of NF-κB using the TransAM NF-κB kit (Active Motif, Carlsbad, CA) as described previously (7). Briefly, HREC were pre-treated with Ad-XBP1 or Ad-GFP for 48 h and exposed to TNF-α (10 ng/ml) for 1 or 4 h. Nuclear extracts were applied to a 96-well plate immobilized oligonucleotide containing the NF-κB consensus site (5′-GGGACTTTCC-3′). After incubation, 100 μl of diluted primary antibody was added and incubated for 1 h, followed by incubation with a secondary antibody for another 1 h. The plate was read at 450 nm using a 1420 microplate reader (PerkinElmer Life Sciences). Specificity of the assay was monitored by competition with wild-type or mutated NF-κB consensus oligonucleotide. Experiments were performed in triplicate. Results were normalized by total protein in nuclear extract.

Oligonucleotide Pulldown Assay—Nuclear protein extracts (100 μg) were incubated overnight with oligonucleotides containing NF-κB consensus sequences conjugated previously to agarose beads (Santa Cruz Biotechnology). Purification was performed per the manufacturer's instructions. Protein complexes were eluted in SDS sample buffer and subjected to SDS-PAGE. NF-κB was detected by Western blot analysis. Level of nucleoporin p62 in the nuclear extract was determined as input control. Nuclear level of XBP1 was also examined by Western blot analysis.

Immunocytochemistry—HREC were cultured on collagen I-coated coverslips (BD Biosciences) under the same conditions described above. After desired treatment, HREC were fixed in 4% formaldehyde for 10 min and permeabilized with 0.5% Triton X-100 in PBS for 5 min. Staining were performed by blocking with 10% normal goat serum for 1 h followed by incubating with mouse anti-ICAM-1 and anti-VCAM-1 antibodies (5 μg/ml, Hybridoma Bank, Iowa City, IA) overnight at 4 °C. Then, cells were incubated with Cy3 goat anti-mouse antibody (1:200, Molecular Probes, Invitrogen), and nuclei were stained with VECTASHIELD mounting medium with DAPI (Vector Laboratories, Inc, Burlingame, CA). NF-κB distributions were stained by Cellomics NF-κB Activation HitKit HSC Reagent kit (Thermo Fisher Scientific) as described previously (30). Stained cells were observed and photographed under a Olympus Provis AX-70 fluorescent microscope (Olympus). Images presented were from three independent experiments.

Statistical Analysis—The quantitative data were presented as mean ± S.D. Statistical analyses were performed using one-way analysis of variance with Bonferroni's multiple comparison test. Statistical differences were considered significant at a p value of < 0.05.

RESULTS

Preconditioning with ER Stress Suppressed Endothelial Adhesion Molecule Expression in Response to TNF-α—Induction of adhesion molecule expression in endothelial cells by inflammatory cytokines such as TNF-α is a central step in the pathogenesis of BRB dysfunction and retinal vascular leakage. We determined whether ER stress preconditioning affects TNF-α-induced ICAM-1 and VCAM-1 expression in retinal endothelial cells. ER stress preconditioning was achieved by pretreatment of primary HREC with a very low dose of tunicamycin (0.1 μg/ml) for 8 h. Cells were then exposed to TNF-α (10 ng/ml) for 4 or 24 h. mRNA expressions of adhesion molecules were examined at 4 h after TNF-α treatment, whereas protein levels were measured at both time points. We found that ICAM-1 and VCAM-1 mRNA expression was up-regulated 10- and 8.5-fold, respectively, after TNF-α treatment. The up-regulation was significantly attenuated in cells pretreated with tunicamycin (Fig. 1*A*). In parallel, immunocytochemistry shows robustly increased expression of ICAM-1 and VCAM-1 in TNF-α-treated cells, which was markedly reduced by tunicamycin pretreatment (Fig. 1, *B* and *C*). In parallel, results from Western blot analysis further confirmed the reduction of ICAM-1 and VCAM-1 protein levels in preconditioned cells (Fig. 1, *D*–*G*). Notably, ICAM-1 and VCAM-1, like other cell surface adhesion molecules, are glycoproteins that contain carbohydrate chains covalently attached to asparagines (*N*-glycan) or serine/theronine (*O*-glycan) residues. TNF-α-induced increase in glycosylated ICAM-1 and VCAM-1 were completely abolished by pretreatment with tunicamycin, an inhibitor of *N*-glycosylation,

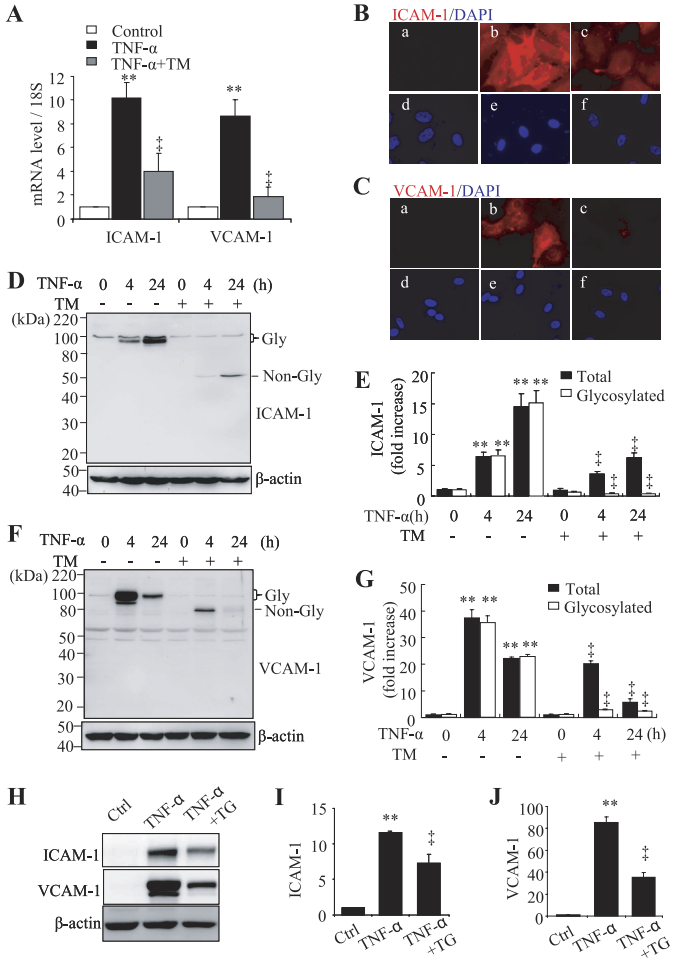

FIGURE 1. **ER stress preconditioning suppressed TNF-α-induced ICAM-1 and VCAM-1 expression in HREC.** HREC were preincubated with 0.1 μg/ml tunicamycin (*TM*; *A–G*) or 10 nM thapsigargin (*TG*; *H–J*) for 8 h followed by exposure to 10 ng/ml TNF-α for 4h or 24 h. *A*, the mRNA level of ICAM-1 and VCAM-1 was measured by real-time RT-PCR in tunicamycin-preconditioned HREC after TNF-α treatment for 4 h. *B* and *C*, expression of ICAM-1 (*B*) and VCAM-1 (*C*) was analyzed by immunocytochemistry in tunicamycin-preconditioned HREC after TNF-α treatment for 24 h. Results show that ICAM-1 (*B*, *a*) and VCAM-1 (*C*, *a*) were expressed at low levels in unstimulated HREC but robustly increased after TNF-α treatment (*B*, *b* and *C*, *b*). Pretreatment with TM markedly inhibited TNF-α-induced ICAM-1 (*B*, *c*) and VCAM-1 (*C*, *c*) expression. *D–G*, expression of ICAM-1 (*D*) and VCAM-1 (*F*) was determined by Western blot analysis in tunicamycin-preconditioned HREC after TNF-α treatment for 4 and 24 h and semiquantified by densitometry (*E* and *G*). *H–J*, expression of ICAM-1 and VCAM-1 in thapsigargin-preconditioned HREC were detected by Western blot analysis after TNF-α treatment for 24 h and semiquantified by densitometry (*I* and *J*). **, $p < 0.01$ *versus* control and ‡, $p < 0.01$ *versus* TNF-α. *Ctrl*, control.

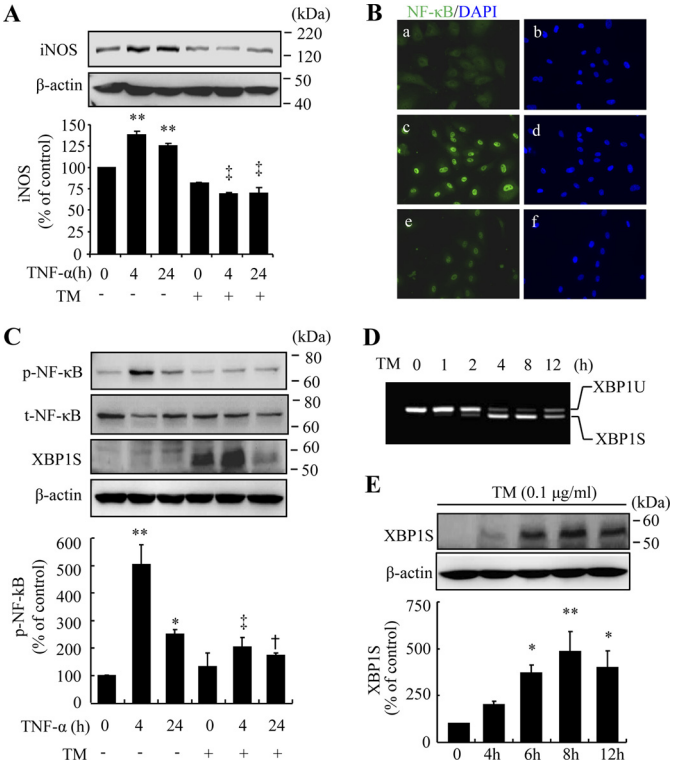

FIGURE 2. **ER stress preconditioning alleviated inducible nitric oxide synthase expression and inhibited NF-κB activation in HREC.** *A*, HREC was pretreated with 0.1 μg/ml tunicamycin (*TM*) for 8 h followed by exposure to 10 ng/ml TNF-α for 4 or 24 h. inducible nitric oxide synthase (*iNOS*) expression were determined by Western blot analysis. *B*, nuclear translocation of NF-κB detected by immunocytochemistry in HREC after TNF-α treatment for 1 h. *B*, *a–b*, Control; *B*, *c–d*, TNF-α; *B*, *e–f*, TNF-α+TM. *C*, phosphorylation of NF-κB p65 subunit at Ser^{536} was determined by Western blot analysis. *, $p < 0.05$; **, $p < 0.01$ *versus* control; †, $p < 0.05$, ‡, $p < 0.01$ *versus* TNF-α. *D* and *E*, XBP1 splicing determined by RT-PCR (*D*) and Western blot analysis (*E*) in HREC after 0.1 μg/ml tunicamycin treatment for the indicated period. *XBP1U*, unspliced XBP1; *XBP1S*, spliced XBP1. *, $p < 0.05$; **, $p < 0.01$ *versus* control.

whereas a new band with molecular mass of 55 kDa (ICAM-1) and 80 kDa (VCAM-1) appeared in tunicamycin-pretreated cells, indicating deglycosylation of ICAM-1 and VCAM-1 by tunicamycin (Fig. 1, *D* and *F*) (29, 32). In addition, levels of total ICAM-1 and VCAM-1 (glycosylated and unglycosylated) were significantly decreased in tunicamycin-pretreated cells, corroborating the reduction in their mRNA expression, suggesting that inhibition of adhesion molecule expression by tunicamycin pretreatment is independent of glycosylation. To further exclude the nonspecific effects of tunicamycin, we tested the effect of preconditioning using another ER stress inducer thapsigargin. Pretreatment of HREC with thapsigargin significantly attenuated TNF-α-induced up-regulation of ICAM-1 and VCAM-1 (Fig. 1, *H–J*), suggesting that ER stress preconditioning suppresses adhesion molecule expression in retinal endothelial cells.

ER Stress Preconditioning Activates XBP1 and Attenuates TNF-α-induced NF-κB Activation—Inducible nitric oxide synthase is a proinflammatory factor and plays a role in ICAM-1 up-regulation in endothelial cells. Zheng *et al.* (33) and Leal *et al.* (34) independently reported that genetic depletion of inducible nitric oxide synthase effectively prevented and inhibited retina ICAM-1 expression, leukostasis, and BRB breakdown in the streptozotocin-induced diabetic mice. Exposure of HREC to TNF-α increased inducible nitric oxide synthase expression, and this increase was abolished in cells pretreated with tunicamycin (Fig. 2*A*), suggesting that inducible nitric oxide synthase inhibition may, at least in part, contribute to the reduced adhesion molecule expression in preconditioned endothelial cells.

NF-κB (nuclear factor κB) is a key transcriptional factor of inflammatory signaling pathways in endothelial cells. Inhibition of NF-κB reduces leukocyte adhesion and attenuates vascular leakage in the diabetic retina, suggesting a critical role of NF-kB in adhesion molecule regulation and leukostasis in diabetic retinopathy (35). To determine whether precondi-

tioning with ER stress impacts activation of NF-kB in retinal endothelial cells, we first analyzed the translocation of NF-κB from cytoplasm to nucleus using immunocytochemistry. In control cells, NF-κB was modestly expressed and diffusely distributed in the cytoplasm (Fig. 2, *B*, *a*). TNF-α stimulated a translocation of NF-κB from the cytoplasm to the nucleus with an increased intensity of NF-κB signal (Fig. 2, *B*, *c*), which was markedly reduced in tunicamycin-primed cells (Fig. 2, *B*, *e*). In addition, exposure of HREC to TNF-α resulted in phosphorylation of the p65 subunit of NF-κB at Ser^{536}, a crucial step for the transcriptional activation of NF-κB, which was largely prevented by pretreatment with tunicamycin (Fig. 2*C*). These results indicate that ER stress preconditioning reduces NF-κB activation in retinal endothelial cells.

XBP1 is a master regulator of the adaptive UPR in response to ER stress. XBP1 is activated by IRE1 through unconventional splicing of XBP1 mRNA. Spliced XBP1 is a transcription factor that induces ER chaperone genes to ameliorate ER stress. Recent studies suggest that XBP1 is also an important player that regulates immune response (36, 37). We thus determined whether XBP1 is activated by ER stress preconditioning. In cells pretreated with tunicamycin for 8 h, the spliced XBP1 level was significantly increased (Fig. 2*C*). Importantly, at this dosage, tunicamycin had no impact on NF-kB activation (Fig. 2*C*) or ICAM-1/VCAM-1 expression (Fig. 1, *A* and *D*–*G*). Tunicamycin treatment induced a time-dependent XBP1 mRNA splicing in HREC (Fig. 2*D*). The protein level of spliced XBP1 increased from 4 h, peaked at 8 h, and declined at 12 h. These results indicate that XBP1 is activated by ER stress preconditioning in HREC.

XBP1 Inhibition Attenuates Protective Effects of ER Stress Preconditioning on Adhesion Molecule Expression, Leukocyte Adhesion, and NF-kB Activation—We next determined whether XBP1 activation is essential for the inhibitory effects of ER stress preconditioning on adhesion molecule expression. HREC were treated with 0.1 μg/ml tunicamycin for 8 h, in the presence or absence of different dose of quinotrierixin, a specific inhibitor of XBP1 splicing (38). As shown in Fig. 3*A*, splicing of XBP1 mRNA induced by tunicamycin was dose-dependently inhibited by quinotrierixin. Consistently, the protein level of spliced XBP1 was significantly decreased by quinotrierixin at the doses of 0.1 and 1 μM (Fig. 3, *A* and *B*). Pretreatment of HREC with 0.1 μM quinotrierixin significantly attenuated the inhibitory effect of preconditioning on ICAM-1 and VCAM-1 expression in HREC (Fig. 3, *C* and *D*). In addition, ER stress preconditioning significantly alleviated TNF-α-induced leukocyte adhesion to endothelial cells, but this protective effect was markedly reversed by pretreatment of cells with quinotrierixin (Fig. 3*E*). These results suggest that XBP1 activation is essential for the inhibitory effect of ER stress preconditioning on adhesion molecule expression and leukocyte adhesion in HREC.

We next determined whether XBP1 activation is required for inhibition of NF-κB activation by ER stress preconditioning. Interestingly, blockade of XBP1 splicing by quinotrierixin increased NF-κB activation and augmented TNF-α-induced NF-κB activation (Fig. 3*F*). Moreover, XBP1 inhibition reversed the effect of preconditioning on NF-κB phosphorylation induced by TNF-α (Fig. 3*F*), suggesting that XBP1 regulates the basal level as well as TNF-α-stimulated NF-κB activation. To confirm the results from XBP1 inhibitor, XBP1 was knocked down using siRNA in HREC. The knockdown efficiency was determined by intracellular level of spliced XBP1 in the presence of proteasome inhibitor, MG-132, which prevents the proteasomal degradation of XBP1 protein (Fig. 3*G*). The results show that downregulation of XBP1 in-

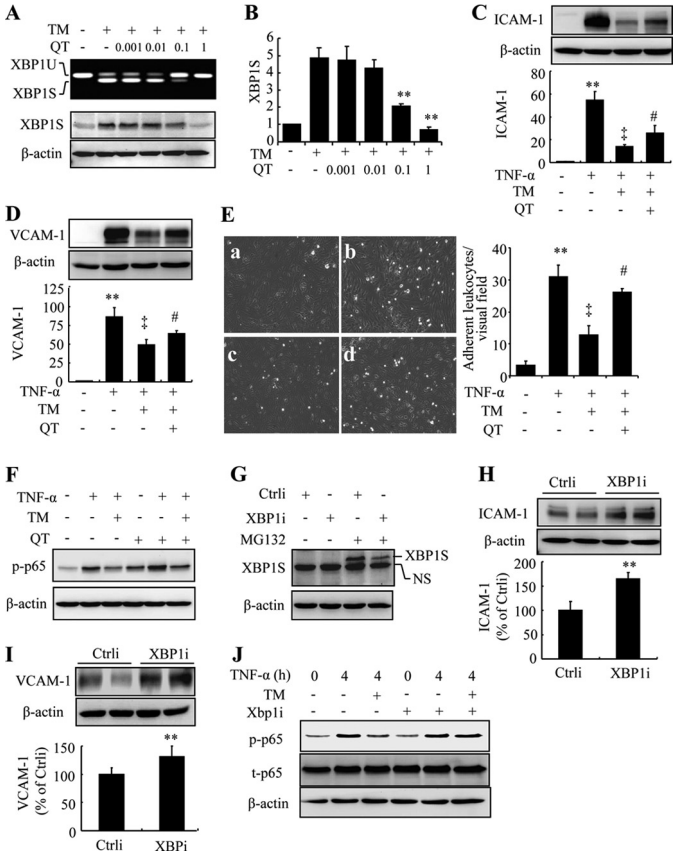

FIGURE 3. **Pharmaceutical and genetic inhibition of XBP1 splicing attenuated the protective effect of ER stress preconditioning in HREC.** *A* and *B*, HREC were incubated with 0.1 μg/ml tunicamycin (*TM*) in presence or absence of quinotrierixin (*QT*) (0.001–1 μM) for 8 h. *A*, spliced XBP1 was determined by RT-PCR (*upper panel*) and Western blot analysis (*lower panel*) using specific antibody against spliced form of XBP1 (*XBP1S*). *B*, protein level of XBP1S was semiquantified by densitometry. **, $p < 0.01$ *versus* control; ‡, $p < 0.01$ *versus* tunicamycin. *C* and *D*, HREC were preincubated with 0.1 μg/ml tunicamycin with or without 0.1 μM quinotrierixin for 8 h followed by treatment with 10 ng/ml TNF-α for 24 h. Expression of ICAM-1 (*C*) and VCAM-1 (*D*) were determined by Western blot analysis and semiquantified by densitometry. **, $p < 0.01$ *versus* control; ‡, $p < 0.01$ *versus* TNF-α; #, $p < 0.05$ *versus* tunicamycin+TNF-α. *E*, *in vitro* leukocyte adhesion assay. HREC were preincubated with 0.1 μg/ml tunicamycin with or without 0.1 μM quinotrierixin for 8 h followed by treatment with 10 ng/ml TNF-α for 4 h, and then THP-1 monocytes were added and co-cultured for 3 h. Adherent monocytes were counted per visual fields and expressed as mean ± S.D. *E*, *a*, Control; *E*, *b*, TNF-α; *E*, *c*, TNF-α+TM; *E*, *d*, TNF-α+TM+QT. **, $p < 0.01$ *versus* control; ‡, $p < 0.01$ *versus* TNF-α; #, $p < 0.05$ *versus* tunicamycin+TNF-α. *F*, HREC were pretreated with 0.1 μg/ml tunicamycin with or without 0.1 μM quinotrierixin for 8 h followed by TNF-α treatment for 4 h. Phosphorylation of NF-κB p65 subunit (Ser^{536}) was determined by Western blot analysis. *G*–*J*, HREC were transfected with XBP1 siRNA for 48 h. The knockdown efficiency was determined by protein level of XBP1S in the presence of MG-132 (10 μM) (*G*). Expression of ICAM-1 (*H*) and VCAM-1 (*I*) were determined by Western blot analysis. *J*, XBP1 siRNA-tranfected cells were pretreated with 0.1 μg tunicamycin for 8 h, followed by TNF-α treatment for 4 h. Phosphorylation of NF-κB p65 (Ser^{536}) was determined. *Ctrli*, control siRNA; *XBP1i*, XBP1 siRNA.

creased ICAM-1 and VCAM-1 expression in HREC (Fig. 3, *H* and *I*). Moreover, the effect of ER stress preconditioning on NF-κB phosphorylation was abolished in cells treated with XBP1 siRNA (Fig. 3*J*). These results collectively suggest that XBP1 activation is an important mediator of the beneficial effects of ER stress preconditioning on inflammatory response in retinal endothelial cells.

Overexpression of Spliced XBP1 Ameliorated TNF-α-induced Adhesion Molecule Expression, Leukocyte Adhesion, and NF-κB Activation—To examine whether XBP1 directly regulates inflammatory response in retinal endothelial cells, we overexpressed spliced XBP1, an active transcription factor, in HREC by infection of cells with adenovirus encoding mouse spliced XBP1 (Ad-XBP1S). Adenovirus encoding GFP (Ad-GFP) were used as control. Forty-eight hours after adenoviral infection, the medium was refreshed with 2% serum-containing medium to allow the cells to reach quiescence, followed by TNF-α treatment for 4 or 24 h. Adhesion molecule expression and NF-κB activation were determined by Western blot analysis. TNF-α induced a robust increase in ICAM-1 and VCAM-1 expression in Ad-GFP-treated cells but not in Ad-XBP1S-treated cells (Fig. 4, *A* and *B*). Consistently, TNF-α-induced leukocyte adhesion was significantly reduced in cells treated with Ad-XBP1S (Fig. 4*C*). These results indicate that activation of XBP1 inhibits endothelial adhesion molecule expression and leukocyte adhesion to endothelial cells.

We next determined whether XBP1 regulates the activation of NF-κB pathway. In Ad-GFP-infected cells, TNF-α treatment induced a rapid phosphorylation of NF-κB (Ser^{536}) at 30 min, 1 h, and 4 h. (Fig. 4*D*) in Ad-GFP-treated cells. Conversely, NF-κB phosphorylation was dramatically attenuated at all time points after TNF-α treatment in Ad-XBP1S-treated cells (Fig. 4*D*). To further confirm the inhibition of NF-κB activation by XBP1, DNA binding capacity and transcriptional activity of NF-κB were determined after TNF-α treatment for 1 h or 4 h in cells preinfected with Ad-GFP or Ad-XBP1S. DNA binding capacity of NF-κB was measured by agarose oligonucleotide pulldown assay. In this assay, nuclear extracts from were incubated with NF-κB-binding oligonucleotides conjugated to agarose beads. Binding of NF-κB to its consensus sequence was determined by Western blot analysis. The results show that TNF-α induced NF-κB binding to its consensus DNA sequence in Ad-GFP-treated cells, and the binding was markedly reduced in Ad-XBP1S-treated cells (Fig. 4*E*). The transcriptional activity of NF-κB was further quantified using TransAM NF-κB activity assay. The results show that NF-κB activity was increased by 2.9- and 3.6-fold after TNF-α treatment for 1 and 4 h, respectively, in Ad-GFP-treated cells. The increases were significantly reduced in Ad-XBP1S-treated cells (Fig. 4*F*). These results suggest that XBP1 inhibits adhesion molecule expression and leukostasis through blockade of NF-κB activation.

XBP1 Inhibits IKK Activation through Feedback Regulation of IRE Phosphorylation and Up-regulation of GRP78—Activation of IκB kinase (IKK) is a critical step in multiple pathways that lead to NF-κB activation. IKK phosphorylates the NF-κB regulatory protein IκB, resulting in proteasomal degradation

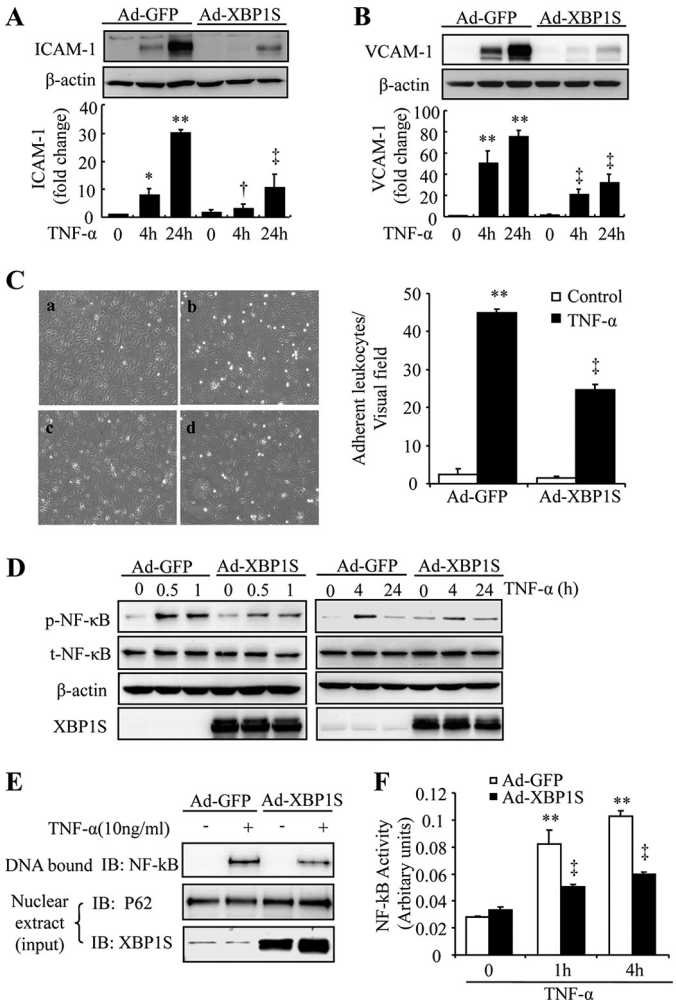

FIGURE 4. **Overexpression of spliced XBP1 inhibited TNF-α-induced ICAM-1 and VCAM-1 and leukocyte adhesion via suppression of NF-κB activation in HREC.** Overexpression of spliced XBP1 was achieved by infection of HREC with adenovirus encoding with the spliced form of XBP1 (*XBP1S*; Ad-XBP1S) at a multiplicity of infection of 20 for 48 h. Adenovirus encoding GFP (Ad-GFP) were used as control. After infection with Ad-GFP and Ad-XBP1S, HREC were treated with 10 ng/ml TNF-α for 0–24 h. Cells were harvested for biochemical assays (*A*, *B*, *D*, *E*, and *F*) or used for leukocyte adhesion assay (*C*). *A* and *B*, expression of ICAM-1 (*A*) and VCAM-1 (*B*) was determined by Western blot (*IB*) analysis and semiquantified by densitometry. *C*, THP-1 monocytes were co-cultured with HREC for 3 h, and adherent monocytes were counted from three different visual fields and expressed at mean ± S.D. *C, a,* Ad-GFP; *C, b*, Ad-GFP+TNF-α; *C, c*, Ad-XBP1S; *C, d*, Ad-XBP1S+TNF-α. *D*, phosphorylation NF-κB p65 (Ser^{536}) was determined in HREC after treatment with TNF-α for 0.5–24 h. *E*, agarose oligonucleotide pulldown assay. Nuclear extract from cells was incubated with agarose beads coated by the NF-κB consensus sequence. After intensive wash, bound NF-κB was determined by Western blot analysis. Level of nuclear membrane protein P62 in the input was used as loading control. *F*, the transcriptional activity of NF-κB was quantified using ELISA-based TransAM NF-κB activity assay. *, $p < 0.05$; **, $p < 0.01$ *versus* Ad-GFP; †, $p < 0.05$; ‡, $p < 0.01$ *versus* Ad-GFP+TNF-α.

of IκB and the release of NF-κB for nuclear translocation (39, 40). In addition, IKK directly phosphorylates p65 subunit of NF-κB at Ser^{536}, Ser^{276}, and Ser^{468}, enhancing the transcriptional activity of NF-κB. To investigate whether XBP1 regulates NF-κB activation via IKK, we determined the effect of XBP1 on TNF-α-induced phosphorylation of IKK. As shown in Fig. 5*A*, TNF-α induced a significant increase in IKK phosphorylation at 5 min, which was gradually diminished within 60 min. Phosphorylation of IKK further induced a rapid and

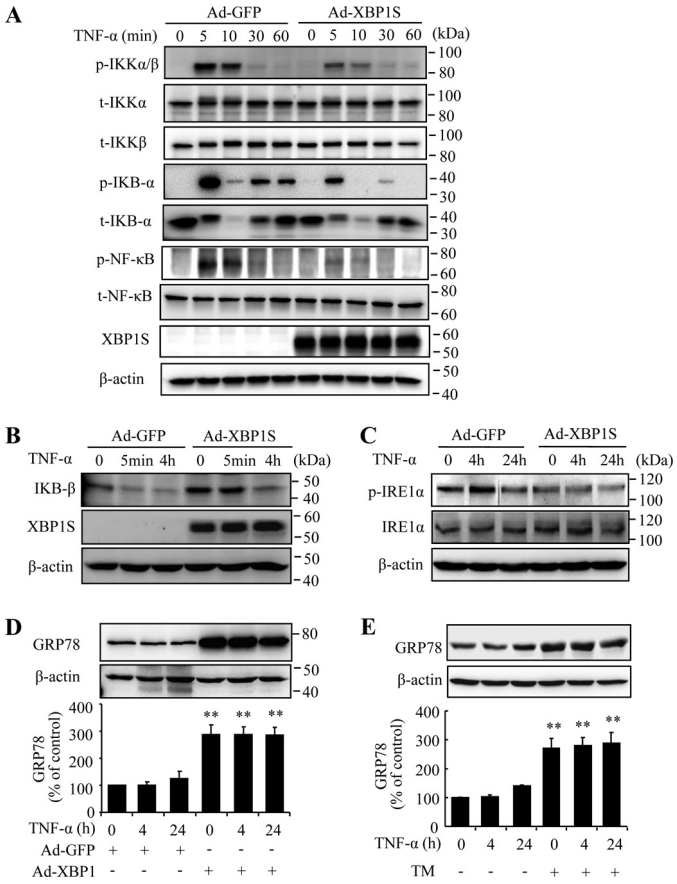

FIGURE 5. **Spliced XBP1 blocked TNF-α induced IKK activation through inhibition of IRE phosphorylation and up-regulation of GRP78.** *A*, HREC were infected with Ad-XBP1S or Ad-GFP for 48 h, followed by treatment with 10 ng/ml TNF-α for up to 60 min. Phosphorylation of IKKα/β at $Ser^{176/180}$, IκB-α at Ser^{32}, and NF-κB at Ser^{536} were detected by Western blot analysis. Total IKKα, IKKβ, IκB-α, and NF-κB were also determined. *p*, phosphorylated; *t*, total. Representative results were from three independent experiments. *B–D*, HREC were infected with Ad-XBP1S or Ad-GFP as described and treated with 10 ng/ml TNF-α for indicated time periods. Expression of IκB-β (*B*), total and phospho-IRE1α (*C*), and GRP78 (*D*) were determined by Western blot analysis. *E*, HREC were pretreated with tunicamycin (*TM*) followed by exposure to TNF-α for 4 and 24 h. Expression of GRP78 were determined by Western blot analysis. **, $p < 0.01$ *versus* Ad-GFP (*D*) or control (*E*).

robust activation of IκBα indicated by its phosphorylation at Ser^{32}, and a phosphorylation of NF-κB p65 subunit at Ser^{536}. All of these changes are remarkably suppressed in Ad-XBP1S-treated cells. In addition, overexpressing XBP1 increases total level of IκBβ and partially reversed the reduction in IκBβ induced by prolonged TNF-α treatment (Fig. 5*B*), which may in part contribute to inhibition of NF-κB activation by XBP1.

To further address how XBP1 regulates IKK activation, we determined IRE1α in both resting and TNF-α-stimulated cells. Several recent studies suggest that IRE1α is required for TNF-α-induced IKK activation (39). In addition, depletion of XBP1 leads to overactivation of IRE1α under stress conditions (37). Thus, it is possible that XBP1 regulates IKK and NF-κB activation through IRE1α. We found that overexpression of spliced XBP1 resulted in a decreased basal level of IRE1α activation in HREC. Moreover, XBP1 prevented TNF-α-induced IRE1α activation but did not alter the total level of IRE1α (Fig. 5*C*). In addition, XBP1 significantly increases expression of the 78-kDa glucose-regulated protein GRP78, a major ER chaperone that ameliorates ER stress and IRE1α activation. These results suggest that increased GRP78 expression by XBP1 may be responsible for inhibition of IRE1α, IKK, and NF-κB activation and adhesion molecule expression induced by TNF-α in retinal endothelial cells.

ER Stress Preconditioning Prevents TNF-α-induced Adhesion Molecule Expression, Leukostasis, and Vascular Leakage in Mouse Retinas—Finally, we determined the *in vivo* effect of ER stress preconditioning on TNF-α-induced retinal inflammation and vascular leakage. ER stress preconditioning was achieved by periocular injection of a very low dose of tunicamycin (10 ng/eye) for 12h, followed by an intravitreal injection of TNF-α to induce retinal inflammation. Adhesion molecule expression, leukostasis and vascular permeability were measured at 24 h after intravitreal injection of TNF-α. The results show that intravitreal injection of TNF-α induced significantly increased adhesion molecule expression in the retina, which was almost completed abolished by ER stress preconditioning (Fig. 6, *A–D*). Notably, preconditioning with tunicamycin induced a significant increase in XBP1 activation but did not affect retinal adhesion molecule expression (data not shown). Moreover, TNF-α stimulated leukocytes adhere to retinal endothelial cells in control eyes but not in tunicamycin-preconditioned eyes (Fig. 6, *E* and *F*). In parallel, retinal vascular permeability was increased after TNF-α treatment and reduced by ER stress preconditioning. These results strongly suggest that ER stress preconditioning could provide beneficial effect in mitigating retinal inflammation and vascular damage by enhancing the protective system of ER mediated by XBP1.

DISCUSSION

Leukocyte-endothelial adhesion and interaction has been recognized as an early and rate-limiting step in the process of acute and chronic inflammatory response associated with many vascular diseases including atherosclerosis and diabetic retinopathy. In a rat model of diabetes induced by streptozotocin, leukocyte stasis (leukostasis) in retinal vasculature increased 3.2-fold as early as 1 week after diabetes induction, correlated with breakdown of the BRB and retinal capillary nonperfusion (11, 12, 18). Inhibition of adhesion molecule expression or bioactivity in endothelial cells or leukocytes not only prevents leukostasis but also ameliorates endothelial dysfunction, BRB breakdown, and vascular cell death (11, 12, 18). These findings suggest that regulation of adhesion molecules is a potential target for treatment of diabetic complications. In the present study, we demonstrate that preconditioning with ER stress protects retinal endothelial cells from inflammatory cytokine-induced adhesion molecule expression, leukocyte adhesion, and vascular leakage in the retina. Moreover, our results indicate that activation of XBP1, a major regulator of the adaptive response to ER stress, is essential to the beneficial effects of ER stress preconditioning through regulation of the IRE1α/IKK/NF-κB pathway. This study for the first time elucidates an important role of endogenous protective mechanism of the ER in regulation of endothelial function and inflammatory response in the retinal vascular system.

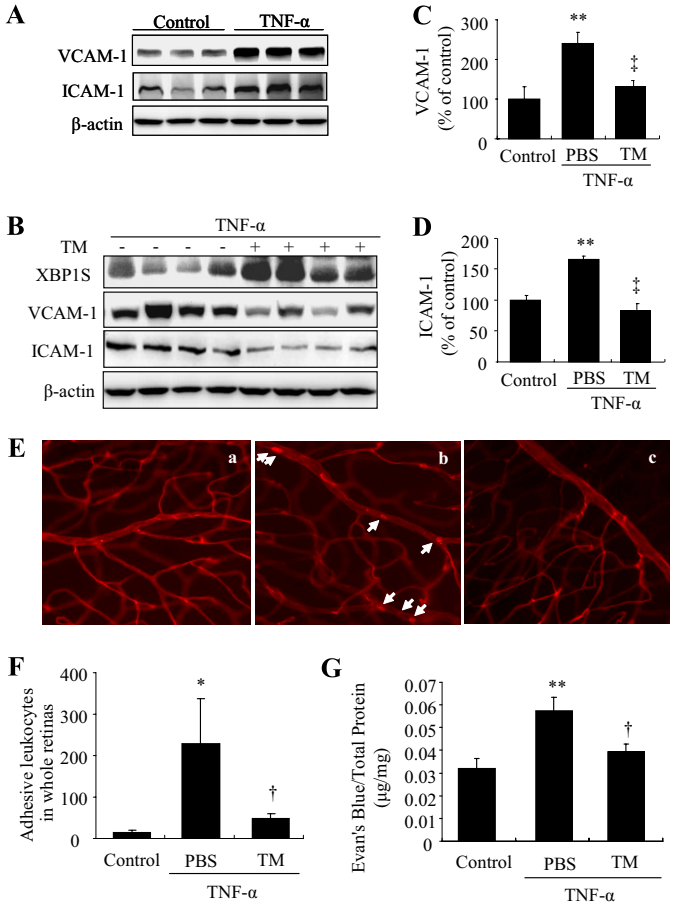

FIGURE 6. **Preconditioning with ER stress reduces adhesion molecule expression, ameliorates leukostasis, and alleviates vascular leakage in mouse retinas.** Eight-week-old C57BL/6J mice received a periocular injection of tunicamycin (*TM*, 10 ng/eye) in one eye and vehicle in the contralateral eye. Twelve hours later, mice were given an intravitreal injection of TNF-α (1 pmol/eye) or PBS as control in both eyes. Retinal adhesion molecule expression, leukostasis, and vascular permeability were measured 24 h after TNF-α injection. *A–D*, retinal expression of VCAM-1, ICAM-1, and XBP1S was determined by Western blot analysis and semiquantified by densitometry. **, $p < 0.01$ *versus* control; ‡, $p < 0.01$ *versus* TNF-α ($n = 4$ in all groups). *E*, representative images of retinal leukostasis analyzed by concanavalin A-lectin staining. *E*, *a*, control; *E*, *b*, TNF-α; *E*, *c*, TNF-α with tunicamycin preconditioning. *F*, quantification of adherent leukocytes per retina (mean ± S.D.). *, $p < 0.05$ *versus* control; †, $p < 0.05$ *versus* TNF-α ($n = 3$ in all groups). *G*, retinal vascular leakage was measured by Evan's blue-albumin method. Results were expressed microgram of extravascular Evan's blue per milligram of total retinal protein. **, $p < 0.01$ *versus* control; †, $p < 0.05$ *versus* TNF-α ($n = 5$ in control group, $n = 10$ in groups of TNF-α or TNF-α with tunicamycin preconditioning).

ICAM-1 and VCAM-1 are the most well characterized adhesion molecules and are key players in the process of leukocyte-endothelial adhesion. ICAM-1 mediates leukocyte-endothelial adhesion by binding to leukocyte function-associated antigen (LFA-1, CD11a/CD18) or macrophage-1 antigen (Mac-1, CD11b/CD18) that are expressed on leukocytes, whereas VCAM-1 promotes leukocytes binding through interaction with cognate receptor integrin $\alpha 4\beta 1$ (VLA-4) (16). Binding of leukocytes to either ICAM-1 or VCAM-1 induces multiple effects in endothelial cells, including clustering of adhesion molecules, rearrangement of the cytoskeleton, and activation of intracellular signaling leading to oxidative stress and enhanced inflammatory response (16, 41). Our results show that ICAM-1 and VCAM-1 are expressed at low levels in resting retinal endothelial cells and up-regulated by 15-fold (ICAM-1) or more than 35-fold (VCAM-1) upon stimulation with inflammatory cytokine TNF-α. TNF-α is a potent inducer of ER stress and the UPR through increasing reactive oxygen species production (42). Intriguingly, pretreatment with tunicamycin suppresses TNF-α-induced reactive oxygen species generation and cell death, suggesting that activation of the UPR is sufficient to counteract the detrimental effect of TNF-α on oxidative stress and cell death (42). In the present study, we demonstrate that ER preconditioning significantly attenuated TNF-α-induced ICAM-1 and VCAM-1 expression. Notably, ICAM-1 and VCAM-1 are both transmembrane glycoproteins. The cDNA of ICAM-1 encodes a core protein of 505 amino acids with predicted molecular mass of 58 kDa, and the mature protein, however, has a molecule mass ranging from 80–114 kDa depending on the degree of glycosylation (32). Similarly, mature VCAM-1 has a molecule mass of 102 kDa, whereas the nonglycosylated protein is 81 kDa. As tunicamycin functions as an inhibitor of *N*-glycosylation, we observed that pretreatment of HREC with tunicamycin suppresses ICAM-1 and VCAM-1 glycosylation (shift of molecular mass from 97–100 kDa to 55 kDa for ICAM-1 and from 100 kDa to 80 kDa for VCAM-1). However, preconditioning with tunicamycin significantly decreases the mRNA as well as total protein levels of ICAM-1 and VCAM-1, suggesting that the inhibitory effect of preconditioning on adhesion molecules is independent of glycosylation. Furthermore, pretreatment of cells with thapsigargin also inhibits TNF-α-induced ICAM-1 and VCAM-1 up-regulation. These results together imply a role of ER stress preconditioning in regulation of adhesion molecule expression.

Recent studies suggest that the IRE1/XBP1 pathway, the most conserved UPR branch, is actively involved in regulation of immune response (36, 37). Activation of XBP1 by IRE1 induces expression of ER chaperones that reduce ER stress and promote cell survival. In addition, XBP1 is required for ER biogenesis and the development of a number of immune cells, such as plasma cells, dentritic cells, and Paneth cells. Mouse embryonic fibroblasts deficient of XBP-1 mounted stronger ER stress and JNK activation when compared with wild-type cells (43). Consistently, in heterozygous XBP1 knock-out mice (lack one allele of XBP1) fed with a high-fat diet, the liver and adipose tissues showed increased ER stress and JNK activation, coupled with insulin resistance (43). In addition, recent work by Kaser and colleagues (37) demonstrates that deletion of XBP1 in intestinal epithelial cells results in spontaneous small intestinal mucosal inflammation accompanied by increased ER stress and enhanced susceptibility to inflammation induced by inflammatory stimuli, such as bacterial products (flagellin) and TNF-α. In the present study, we found that down-regulation of XBP1 induces increased expression of adhesion molecules in retinal endothelial cells, suggesting that XBP1 is essential for maintaining a low inflammatory state in resting endothelial cells. Inhibition of XBP1 splicing by quinotrierixin or knockdown of XBP1 by siRNA blocks the inhibitory effect of ER stress

preconditioning on NF-κB-mediated ICAM-1 and VCAM-1 up-regulation. Moreover, overexpression of spliced XBP1 suppresses TNF-α-induced NF-κB activation, adhesion molecule expression, and leukocyte adhesion. These results strongly suggest that XBP1 activation is required for the inhibitory effect of ER stress preconditioning on endothelial inflammation. In addition, we found that spliced XBP1 negatively regulates IRE1 activation, an essential step for TNF-α-induced IKK and NF-κB activation, in both unstimulated and TNF-α-stimulated cells. These results corroborate previous findings from Kazer *et al.* (37) showing that depletion of XBP1 leads to overactivation of IRE1α. However, the mechanisms by which XBP1 regulates IRE1 activation remain to be investigated.

GRP78 is a most abundant ER chaperone that is induced by XBP1 and ATF6 during ER stress. The role of GRP78 in ER stress preconditioning has been controversial. One study demonstrated that GRP78 could contribute to the protective effect of ER stress preconditioning in renal epithelial cells against oxidative injury (31); other studies, however, showed that exogenous GRP78 or the conditioned medium from ER stress-primed cells containing high levels of GRP78 failed to attenuate MCP-1 expression and NF-κB activation in IL-1β- or TNF-α-stimulated cells (24). In the present study, we found that GRP78 is up-regulated by ER stress preconditioning as well as by overexpression of spliced XBP1, suggesting that up-regulation of GRP78 by XBP1 may contribute to the action of ER stress preconditioning. The role of other UPR branches such as activating transcription factor 6 (ATF6) in ER stress preconditioning also warrants investigation in the future.

Taken together, our study demonstrates that preconditioning with ER stress ameliorates retinal endothelial cell adhesion molecule expression, leukocyte-endothelial adhesion, and consequent BRB breakdown, a common feature of diabetic retinopathy. Activation of XBP1 is required for the protective effects of ER stress precondition and is sufficient to inhibit TNF-α-induced inflammation mediated by the IRE1/IKK/NF-κB pathway. Identifying small molecules that enhance XBP1-mediated protective UPR signaling may provide a novel therapeutic strategy for inflammatory retinal diseases, including diabetic retinopathy.

Acknowledgments—We thank Drs. Laurie Glimcher and Ann-Hwee Lee (Harvard School of Public Health, Boston, MA) for adenoviral vectors of XBP1, Dr. Etsu Tashiro (Keio University, Japan) for quinotrierixin, and Diabetes COBRE (Centers of Biomedical Research Excellence) Histology Core (University of Oklahoma Health Sciences Center, Oklahoma City, Oklahoma) for image acquisition.

REFERENCES

1. Klein, R., Klein, B. E., and Moss, S. E. (1992) *Diabetes Care* **15,** 1875–1891
2. Klein, R., Klein, B. E., Moss, S. E., and Cruickshanks, K. J. (1995) *Ophthalmology* **102,** 7–16
3. Miller, J. W., Adamis, A. P., and Aiello, L. P. (1997) *Diabetes Metab. Rev.* **13,** 37–50
4. De La Cruz, J. P., González-Correa, J. A., Guerrero, A., and de la Cuesta, F. S. (2004) *Diabetes-Metab. Res. Rev.* **20,** 91–113
5. Gardner, T. W., and Antonetti, D. A. (2008) *Curr. Diab. Rep.* **8,** 263–269
6. Zhang, S. X., Ma, J. X., Sima, J., Chen, Y., Hu, M. S., Ottlecz, A., and Lambrou, G. N. (2005) *Am. J. Pathol.* **166,** 313–321
7. Li, J., Wang, J. J., Chen, D., Mott, R., Yu, Q., Ma, J. X., and Zhang, S. X. (2009) *Exp. Eye Res.* **89,** 71–78
8. Li, J., Wang, J. J., Yu, Q., Wang, M., and Zhang, S. X. (2009) *FEBS Lett.* **583,** 1521–1527
9. Adamis, A., and Berman, A. (2008) *Seminars in Immunopathology* **30,** 65–84
10. Aiello, L. P., and Wong, J. S. (2000) *Kidney Int. Suppl.* **77,** S113–119
11. Joussen, A. M., Poulaki, V., Mitsiades, N., Kirchhof, B., Koizumi, K., Döhmen, S., and Adamis, A. P. (2002) *FASEB J.* **16,** 438–440
12. Joussen, A. M., Poulaki, V., Le, M. L., Koizumi, K., Esser, C., Janicki, H., Schraermeyer, U., Kociok, N., Fauser, S., Kirchhof, B., Kern, T. S., and Adamis, A. P. (2004) *FASEB J.* **18,** 1450–1452
13. McLeod, D. S., Lefer, D. J., Merges, C., and Lutty, G. A. (1995) *Am. J. Pathol.* **147,** 642–653
14. Funatsu, H., Noma, H., Mimura, T., Eguchi, S., and Hori, S. (2009) *Ophthalmology* **116,** 73–79
15. Tang, S., and Le-Ruppert, K. C. (1995) *Graefes. Arch. Clin. Exp. Ophthalmol.* **233,** 21–25
16. Norman, M. U., James, W. G., and Hickey, M. J. (2008) *J. Leukoc. Biol.* **84,** 68–76
17. Ramos, C. L., Huo, Y., Jung, U., Ghosh, S., Manka, D. R., Sarembock, I. J., and Ley, K. (1999) *Circ. Res.* **84,** 1237–1244
18. Joussen, A. M., Doehmen, S., Le, M. L., Koizumi, K., Radetzky, S., Krohne, T. U., Poulaki, V., Semkova, I., and Kociok, N. (2009) *Mol. Vis.* **15,** 1418–1428
19. Behl, Y., Krothapalli, P., Desta, T., DiPiazza, A., Roy, S., and Graves, D. T. (2008) *Am. J. Pathol.* **172,** 1411–1418
20. Yoneda, T., Imaizumi, K., Oono, K., Yui, D., Gomi, F., Katayama, T., and Tohyama, M. (2001) *J. Biol. Chem.* **276,** 13935–13940
21. Inagi, R., Kumagai, T., Nishi, H., Kawakami, T., Miyata, T., Fujita, T., and Nangaku, M. (2008) *J. Am. Soc. Nephrol.* **19,** 915–922
22. Peyrou, M., and Cribb, A. E. (2007). *Toxicol. In Vitro* **21,** 878–886
23. Hayakawa, K., Hiramatsu, N., Okamura, M., Yao, J., Paton, A. W., Paton, J. C., and Kitamura, M. (2008) *Biochem. Biophys. Res. Commun.* **365,** 47–53
24. Hayakawa, K., Hiramatsu, N., Okamura, M., Yamazaki, H., Nakajima, S., Yao, J., Paton, A. W., Paton, J. C., and Kitamura, M. (2009) *J. Immunol.* **182,** 1182–1191
25. Zhang, S. X., Sima, J., Wang, J. J., Shao, C., Fant, J., and Ma, J. X. (2005) *Curr. Eye Res.* **30,** 681–689
26. Mori, K., Gehlbach, P., Ando, A., Wahlin, K., Gunther, V., McVey, D., Wei, L., and Campochiaro, P. A. (2002) *Invest Ophthalmol. Vis. Sci.* **43,** 2462–2467
27. Lee, A. H., Scapa, E. F., Cohen, D. E., and Glimcher, L. H. (2008) *Science* **320,** 1492–1496
28. Li, J., Wang, J. J., Yu, Q., Chen, K., Mahadev, K., and Zhang, S. X. (2010) *Diabetes* **59,** 1528–1538
29. Lin, J. H., Li, H., Yasumura, D., Cohen, H. R., Zhang, C., Panning, B., Shokat, K. M., Lavail, M. M., and Walter, P. (2007) *Science* **318,** 944–949
30. Li, J., Wang, J. J., Chen, D., Mott, R., Yu, Q., Ma, J. X., and Zhang, S. X. (2009) *Exp. Eye Res.* **89,** 71–78
31. Hung, C. C., Ichimura, T., Stevens, J. L., and Bonventre, J. V. (2003) *J. Biol. Chem.* **278,** 29317–29326
32. Mullins, R. F., Skeie, J. M., Malone, E. A., and Kuehn, M. H. (2006) *Mol. Vis.* **12,** 224–235
33. Zheng, L., Du, Y., Miller, C., Gubitosi-Klug, R. A., Ball, S., Berkowitz, B. A., and Kern, T. S. (2007) *Diabetologia* **50,** 1987–1996
34. Leal, E. C., Manivannan, A., Hosoya, K., Terasaki, T., Cunha-Vaz, J., Ambrósio, A. F., and Forrester, J. V. (2007) *Invest. Ophthalmol. Vis. Sci.* **48,** 5257–5265
35. Kern, T. S. (2007) *Exp. Diabetes Res.* **2007,** 95103
36. Todd, D. J., Lee, A. H., and Glimcher, L. H. (2008) *Nat. Rev. Immunol.* **8,** 663–674

37. Kaser, A., Lee, A. H., Franke, A., Glickman, J. N., Zeissig, S., Tilg, H., Nieuwenhuis, E. E., Higgins, D. E., Schreiber, S., Glimcher, L. H., and Blumberg, R. S. (2008) *Cell* **134,** 743–756
38. Kawamura, T., Tashiro, E., Shindo, K., and Imoto, M. (2008) *J. Antibiot.* **61,** 312–317
39. Hu, P., Han, Z., Couvillon, A. D., Kaufman, R. J., and Exton, J. H. (2006) *Mol. Cell. Biol.* **26,** 3071–3084
40. Bayat, H., Xu, S., Pimentel, D., Cohen, R. A., and Jiang, B. (2008) *Arterioscler. Thromb. Vasc. Biol.* **28,** 127–134
41. Shestakova, M. V., Kochemasova, T. V., Gorelysheva, V. A., Osipova, T. V., Polosukhina, E. P., Baryshnikov, A., and Dedov, II. (2002) *Ter. Arkh.* **74,** 24–27
42. Xue, X., Piao, J. H., Nakajima, A., Sakon-Komazawa, S., Kojima, Y., Mori, K., Yagita, H., Okumura, K., Harding, H., and Nakano, H. (2005) *J. Biol. Chem.* **280,** 33917–33925
43. Ozcan, U., Cao, Q., Yilmaz, E., Lee, A. H., Iwakoshi, N. N., Ozdelen, E., Tuncman, G., Görgün, C., Glimcher, L. H., and Hotamisligil, G. S. (2004) *Science* **306,** 457–461